HHS Public Access

Author manuscript

Org Lett. Author manuscript; available in PMC 2017 November 30.

Published in final edited form as:

Org Lett. 2017 April 07; 19(7): 1820–1823. doi:10.1021/acs.orglett.7b00587.

Enantioselective Synthesis of Dilignol Model Compounds and Their Stereodiscrimination Study with A Dye-Decolorizing Peroxidase

Gaochao Huang[a], **Ruben Shrestha**[a], **Kaimin Jia**[a], **Brian V. Geisbrecht**[b], and **Ping Li**[a,*]

[a]Department of Chemistry, Kansas State University, Manhattan, KS 66506, USA

[b]Biochemistry and Molecular Biophysics, Kansas State University, Manhattan, KS 66506, USA

Abstract

A 4-step enantioselective approach was developed to synthesize *anti* (*1R, 2S*)-**1a** and (*1S, 2R*)-**1b** containing a β-O-4 linkage in good yields. A significant difference was observed for the apparent binding affinities of four stereospecific lignin model compounds with *Tc*DyP by surface plasmon resonance, which was not translated into a significant difference in enzyme activities. The discrepancy may be attributed to the conformational change involving a loop widely present in DyPs upon H_2O_2 binding.

Graphical abstract

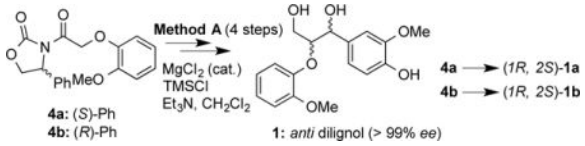

Dye-decolorizing peroxidases (DyPs) are a new family of heme peroxidases that catalyze H_2O_2-dependent oxidation of anthraquinone-based dyes under acidic conditions.[1–3] They have been reported to degrade phenolic lignin model compounds and wheat straw lignocellulose, though the efficiency is low.[4–7] Our interest in DyPs stems from their potential applications in lignin degradation,[8, 9] a critical step in converting lignocellulose biomass to biofuels.[8, 10–13] Lignin biosynthesis produces a β-O-4 interunit linkage up to 50–65% with α and β carbons exhibiting (*R,R*), (*R,S*), (*S,R*), and (*S,S*) stereochemistry.[11, 14] While the lignin polymer is a racemic mixture,[15, 16] studies have suggested that the localized stereochemistry affects its enzymatic digestion.[17–23] However, stereochemical relationships between β-O-4 dilignols and DyPs remained unknown due to limited access to these stereospecific compounds in sufficient amounts.

*Corresponding Author: pli@ksu.edu.

Supporting Information

The Supporting Information is available free of charge on the ACS Publications website at DOI:
Detailed experimental procedures and spectroscopic data (PDF)

Notes

The authors declare no competing financial interest.

While many endeavors had been pursued to synthesize stereospecific lignin model compounds containing a β-O-4 linkage,[21, 24–31] significant progress was not made until recently by Njiojob et al, who had successfully prepared the *syn* (*1S, 2S*)-dilignol using asymmetric epoxidation followed by kinetic resolution.[32] However, attempts to scale up this 9-step reaction resulted in a low yield.[33] Later, the same *syn* compounds were obtained by a 5-step synthesis similar to the method B (Scheme 1) described in this report.[33] However, they had to employ a Mitsunobu reaction to produce *anti* (*1R, 2S*)-dilignol,[33] which resulted in additional three steps and is disadvantageous for reaction scale-up. Thus, we decided to develop a short approach to synthesize *anti* dilignols containing a β-O-4 linkage. Here a 4-step enantioselective approach is reported to prepare *anti* (*1R, 2S*)-**1a** and (*1S, 2R*)-**1b** (Scheme 1), achieving the goal of obtaining all four stereoisomers in gram scales by controlling the conditions of enolate formation in the presence of Evans chiral auxiliaries. These model compounds were studied for their stereodiscrimination by the A-class *Td*DyP from *Thermomonspora curvata* using surface plasmon resonance (SPR) and enzyme activity assays.

As shown in Scheme 1, guaiacol was converted to acid **2** and then reacted with oxazolidinone/thiazolidinethione **3** to yield adduct **4** (Figure 1),[28, 34] which was screened for its efficiency in diastereoselectivity by HPLC. A representative HPLC profile is shown in Figure 2 and the results are summarized in Table 1. For method A involving trimethylsilyl chloride (TMSCl) and catalytic $MgCl_2$,[35, 36] **4a** (X=O, R=*R*-Ph, R´=H) was found to be the best for diastereoselectivity to yield an *anti*-aldol product. When **4a** was reacted with vanillin, di-TMS-protected aldol product was formed initially (see NMR in SI). However, the phenolic TMS was not stable and could be easily cleaved to produce mono-TMS-protected **5a** (X =O, R=*R*-Ph, R´= H). It has to be noted that isolation of the major diastereomer in **5** by silica-gel chromatography was difficult. Therefore, without purification, **5** was directly treated with trifluoroacetic acid (TFA) to afford compound **6**, in which the major diastereomer with *anti*-configuration was isolated in 75% yields. To further optimize diastereoselectivity, effects of organic bases and solvents were also screened. The results are summarized in Table 1. It was concluded that Et_3N and CH_2Cl_2 were the best base and solvent, respectively. It was also found that low temperature slightly improved diastereoselectivity (entries 1 and 2 in Table 1).

Reductive cleavage of the auxiliary in compound **6** with $NaBH_4$ gave the desired stereoisomer, (*1R, 2S*)-**1a** or (*1S, 2R*)-**1b**, depending on the configuration of phenyl group. The enantiomeric excess (*ee*) of the final compounds was determined to be > 99% using chiral HPLC. Assignment of the configurations in each stereoisomer was based on the reported optical rotations, which was also consistent with theoretical predictions.[35, 37] These results are summarized in supplemental Figure S1 and Table S1. Thus, the stereospecific *anti*-dilignols were obtained in just four steps with an overall 42% yield, which was a significant improvement over the other asymmetric methods reported so far.[32, 33]

Method B employing *n*-Bu_2BOTf and DIPEA to form enolates has been recently reported to synthesize *syn*-aldol **7e** (X = O, R = *R*-^{i}Pr, R´ = H) using chiral auxiliary **4e**.[33] However, our screen on auxiliaries found that **4c** had a slightly better diastereoselectivity than **4e (**see Figure S2 and Table S2 in SI). Thus, **4c** was selected as the chiral auxiliary for subsequent

preparations. After the chiral auxiliary in **7** was cleaved by $NaBH_4$ to give **8**, a subsequent hydrogenesis yielded (*1R, 2R*)-**1c** or (*1S, 2S*)-**1d** depending on the configuration of the benzyl (Bn) group in the auxiliary.

Surface plasmon resonance (SPR) is a highly sensitive technique to study non-covalent interactions of biomolecules, especially protein-protein and protein-small molecule interactions in real time.[38] Purified *Tc*DyP (Figure S3 in SI) was immobilized on a CMD500M sensor chip (Xantec Bioanalytics GmbH) via amine coupling chemistry.[39] The synthesized stereoisomers **1a**-**1d** at a series of concentrations were then injected and sensorgrams are shown in supplemental Figure S4. Steady-state affinity analysis based on a 1:1 binding model (Figure S5 in SI) was used to determine the apparent binding affinity (K_D). The results and parameters evaluating global fittings of the data are summarized in Table 2. It was revealed that all stereoisomers had weak interactions with *Tc*DyP. For stereoisomer **1c**, its affinity was too weak to be determined. Among the other three stereoisomers, **1a** appeared to bind the strongest with the enzyme at submillimolar concentrations. The K_D values of **1b** and **1d** are at least 10-fold higher than that of **1a**, suggesting that stereochemistry at C^{α} and C^{β} does affect the substrate binding in the absence of H_2O_2. Such observations may shed light on catalysis by DyPs.

We have previously reported that racemic mixtures of β-O-4 dilignol **1** can be degraded by *Tc*DyP in the presence of H_2O_2.[6] Based on the MS results, C^{α}–C^{β} was proposed to be cleaved during degradation.[6] To investigate the stereochemical effects of *Tc*DyP, the four stereoisomers were individually incubated with the enzyme in the presence of H_2O_2. Reaction rates were determined based on disappearance of the peak at 13.2 min corresponding to the substrate (Figure 3). Specific activities (SAs) of *Tc*DyP toward the four stereoisomers are summarized in Table 2, which are in the order of **1a** > **1d** > **1b** > **1c**, consistent with the order of apparent binding affinities (K_D) obtained by SPR. However, one important difference was found between SPR and enzyme activity assays. It was observed that **1a** bound *Tc*DyP by 14- and 12-fold better than **1b** and **1d**, respectively. Stereoisomer **1c** displayed very weak binding with *Tc*DyP. Therefore, the significant difference observed in SPR experiments was not reflected in enzyme activities toward these stereoisomers, in which only 1.6-fold difference was observed for the ones with the highest (**1a**) and lowest (**1c**) activities.

We recently determined the crystal structure of *Tc*DyP,[40] which revealed that a large loop consisting of residues 277-310 is present next to an access channel leading to the propionate group on pyrrole ring C in the heme active site (Figure 4). The entrance of this channel in D-class DyP from *Bjerkandera adusta* has been shown to be a substrate binding site.[41] The same propionate group has also been demonstrated to provide a direct electron transfer from the substrate to porphyrin radical in heme-containing manganese and ascorbate peroxidases.[42, 43] Additionally, this 34-residue loop is close to W263, which has been characterized as a surface-exposed substrate oxidation site in *Tc*DyP.[40] The closest distance between the loop (L279) and W263 is 6.1 Å. Moreover, this loop is widely present in DyPs although the size varies between classes. Deletion of the loop in *Tc*DyP has resulted in the loss of enzyme activity (data not shown). Thus, it is highly possible that DyP enzymes undergo a conformational change involving this large loop upon H_2O_2 binding. Such H_2O_2-

induced conformational changes have been reported for a number of other heme peroxidases including cytochrome c peroxidase and horseradish peroxidase.[44–48] Since our SPR experiments were carried out in the absence of H_2O_2, the significant difference in K_D with the four stereoisomers may not be translated into a significant difference in enzyme activities toward them, though the overall order of stereochemical preference is retained in both SPR and activity assay experiments.

In summary, a 4-step enantioselective method has been developed to prepare *anti* (*1R, 2S*)-**1a** and (*1S, 2R*)-**1b** in the presence of TMSCl and catalytic $MgCl_2$, achieving the goal of synthesizing all four stereospecific β-O-4 dilignols in gram scales by controlling conditions of enolate formation. The *Tc*DyP displayed different stereodiscrimination against these stereoisomers in the absence and presence of H_2O_2, which may be attributed to the conformational change involving a loop widely present in DyP enzymes upon H_2O_2 binding. The overall weak stereodiscrimination by DyPs may appear advantageous in their applications as a biocatalyst for lignin degradation, as they will not discriminate the source of biomass that may have different localized stereochemistry.

Supplementary Material

Refer to Web version on PubMed Central for supplementary material.

Acknowledgments

This work was supported by awards to P.L from the pilot project of NIH P30GM110761 and Johnson Cancer Research Center. G.H. is supported by an NIH K-INBRE fellowship under grant number P20GM103418.

References

1. Strittmatter, E., Plattner, DA., Piontek, K. Encyclopedia of Inorganic and Bioinorganic Chemistry. John Wiley and Sons, Ltd; New York: 2011. Dye-Decolorizing Peroxidase (DyP).
2. Sugano Y. Cell Mol Life Sci. 2009; 66:1387–1403. [PubMed: 19099183]
3. Colpa DI, Fraaije MW, van Bloois E. J Ind Microbiol Biot. 2014; 41:1–7.
4. Ahmad M, Roberts JN, Hardiman EM, Singh R, Eltis LD, Bugg TDH. Biochemistry. 2011; 50:5096–5107. [PubMed: 21534568]
5. Brown ME, Barros T, Chang MCY. ACS Chem Biol. 2012; 7:2074–2081. [PubMed: 23054399]
6. Chen C, Shrestha R, Jia K, Gao PF, Geisbrecht BV, Bossmann SH, Shi JS, Li P. J Biol Chem. 2015; 290:23447–23463. [PubMed: 26205819]
7. Min K, Gong G, Woo HM, Kim Y, Um Y. Sci Rep. 2015; 5:8245. [PubMed: 25650125]
8. Brown ME, Chang MCY. Curr Opin Chem Biol. 2014; 19:1–7. [PubMed: 24780273]
9. de Gonzalo G, Colpa DI, Habib MHM, Fraaije MW. J Biotechnol. 2016; 236:110–119. [PubMed: 27544286]
10. Paliwal R, Rawat AP, Rawat M, Rai JPN. Appl Biochem Biotech. 2012; 167:1865–1889.
11. Wong DWS. Appl Biochem Biotech. 2009; 157:174–209.
12. ten Have R, Teunissen PJ. Chem Rev. 2001; 101:3397–413. [PubMed: 11749405]
13. Bugg TD, Ahmad M, Hardiman EM, Singh R. Curr Opin Biotech. 2011; 22:394–400. [PubMed: 21071202]
14. Boerjan W, Ralph J, Baucher M. Annu Rev Plant Biol. 2003; 54:519–546. [PubMed: 14503002]
15. Akiyama T, Magara K, Matsumoto Y, Meshitsuka G, Ishizu A, Lundquist K. J Wood Sci. 2000; 46:414–415.
16. Akiyama T, Sugimoto T, Matsumoto Y, Meshitsuka G. J Wood Sci. 2002; 48:210–215.

17. Gall DL, Kim H, Lu FC, Donohue TJ, Noguera DR, Ralph J. J Biol Chem. 2014; 289:8656–8667. [PubMed: 24509858]
18. Gall DL, Ralph J, Donohue TJ, Noguera DR. Environ Sci Technol. 2014; 48:12454–12463. [PubMed: 25232892]
19. Masai E, Ichimura A, Sato Y, Miyauchi K, Katayama Y, Fukuda M. J Bacteriol. 2003; 185:1768–1775. [PubMed: 12618439]
20. Katayama T, Tsutsui J, Tsueda K, Miki T, Yamada Y, Sogo M. J Wood Sci. 2000; 46:458–465.
21. Hishiyama S, Otsuka Y, Nakamura M, Ohara S, Kajita S, Masai E, Katayama Y. Tetrahedron Lett. 2012; 53:842–845.
22. Sato Y, Moriuchi H, Hishiyama S, Otsuka Y, Oshima K, Kasai D, Nakamura M, Ohara S, Katayama Y, Fukuda M, Masai E. Appl Environ Microbiol. 2009; 75:5195–5201. [PubMed: 19542348]
23. Jonsson L, Karlsson O, Lundquist K, Nyman PO. FEBS Lett. 1990; 276:45–8. [PubMed: 2265710]
24. Yue FX, Lu FC, Sun RC, Ralph J. Chem Eur J. 2012; 18:16402–16410. [PubMed: 23109283]
25. Kawai S, Jensen KA, Bao W, Hammel KE. Appl Environ Microbiol. 1995; 61:3407–3414. [PubMed: 7574649]
26. Forsythe WG, Garrett MD, Hardacre C, Nieuwenhuyzen M, Sheldrake GN. Green Chem. 2013; 15:3031–3038.
27. Kishimoto T, Uraki Y, Ubukata M. Org Biomol Chem. 2005; 3:1067–1073. [PubMed: 15750650]
28. Buendia J, Mottweiler J, Bolm C. Chem Eur J. 2011; 17:13877–13882. [PubMed: 22076640]
29. Li KC, Helm RF. Holzforschung. 2000; 54:597–603.
30. Li KC, Helm RF. J Chem Soc Perkin Trans. 1996; 1:2425–2426.
31. Nakatsubo F, Sato K, Higuchi T. Holzforschung. 1975; 29:165–168.
32. Njiojob CN, Rhinehart JL, Bozell JJ, Long BK. J Org Chem. 2015; 80:1771–1780. [PubMed: 25584871]
33. Njiojob CN, Bozell JJ, Long BK, Elder T, Key RE, Hartwig WT. Chem Eur J. 2016; 22:12506–12517. [PubMed: 27459234]
34. Prashad M, Kim HY, Har D, Repic O, Blacklock TJ. Tetrahedron Lett. 1998; 39:9369–9372.
35. Evans DA, Tedrow JS, Shaw JT, Downey CW. J Am Chem Soc. 2002; 124:392–393. [PubMed: 11792206]
36. Evans DA, Downey CW, Shaw JT, Tedrow JS. Org Lett. 2002; 4:1127–1130. [PubMed: 11922799]
37. Evans DA, Rieger DL, Bilodeau MT, Urpi F. J Am Chem Soc. 1991; 113:1047–1049.
38. Nguyen HH, Park J, Kang S, Kim M. Sensors-BASEL. 2015; 15:10481–10510. [PubMed: 25951336]
39. Johnsson B, Lofas S, Lindquist G. Anal Biochem. 1991; 198:268–277. [PubMed: 1724720]
40. Shrestha R, Chen XJ, Ramyar KX, Hayati Z, Carlson EA, Bossmann SH, Song LK, Geisbrecht BV, Li P. ACS Catal. 2016; 6:8036–8047.
41. Yoshida T, Tsuge H, Hisabori T, Sugano Y. FEBS Lett. 2012; 586:4351–4356. [PubMed: 23159941]
42. Sharp KH, Mewies M, Moody PCE, Raven EL. Nat Struct Biol. 2003; 10:303–307. [PubMed: 12640445]
43. Sundaramoorthy M, Kishi K, Gold MH, Poulos TL. J Biol Chem. 1994; 269:32759–32767. [PubMed: 7806497]
44. Miyazaki C, Takahashi H. FEBS Lett. 2001; 509:111–114. [PubMed: 11734216]
45. Wang X, Wang LK, Wang X, Sun F, Wang CC. Biochem J. 2012; 441:113–118. [PubMed: 21916849]
46. Hassler K, Rigler P, Blom H, Rigler R, Widengren J, Lasser T. Opt Express. 2007; 15:5366–5375. [PubMed: 19532790]
47. Wen F, Dong YH, Feng L, Wang S, Zhang SC, Zhang XR. Anal Chem. 2011; 83:1193–1196. [PubMed: 21261275]
48. Bonagura CA, Bhaskar B, Shimizu H, Li HY, Sundaramoorthy M, McRee DE, Goodin DB, Poulos TL. Biochemistry. 2003; 42:5600–5608. [PubMed: 12741816]

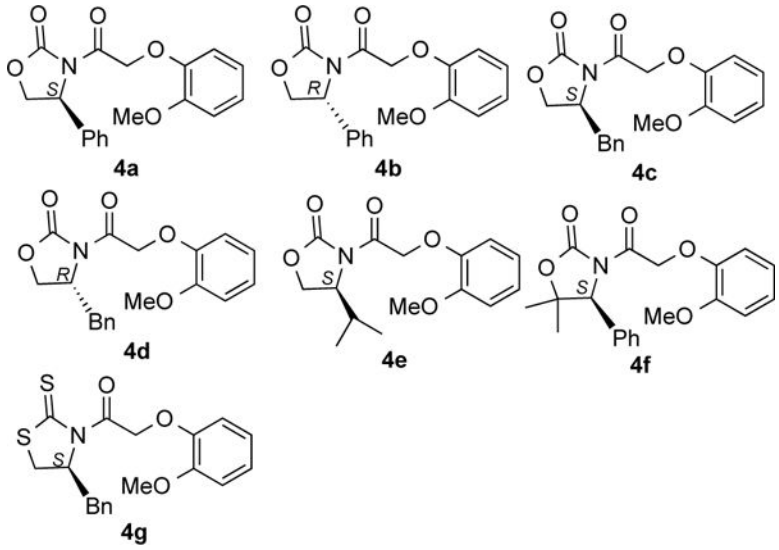

Figure 1.
Structures of **4a–4g** containing Evans auxiliaries

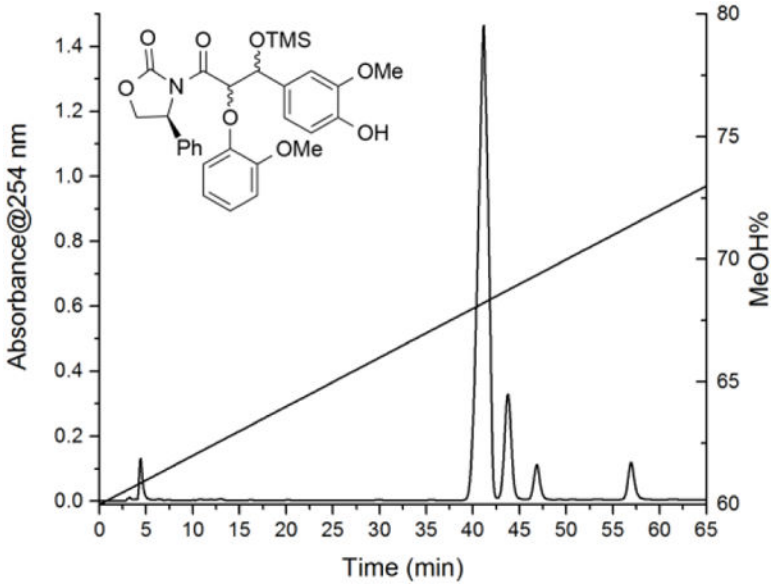

Figure 2.

Representative HPLC profile of diastereoselectivity using method A. The straight line indicates MeOH gradient. The peak at 4.8 min represents unreacted aldehyde.

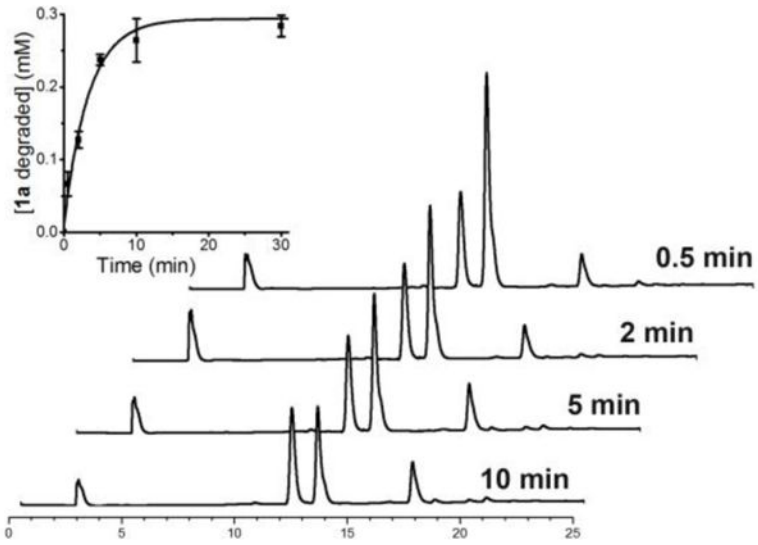

Figure 3.

HPLC profiles of *Tc*DyP incubating with **1a** and H_2O_2. Peaks at 3.1, 12.0, 13.2, and 17.4-20.5 min correspond to impurity from citrate buffer, internal standard, substrate **1a**, and degradation products, respectively. The inset shows the rate of **1a** degradation.

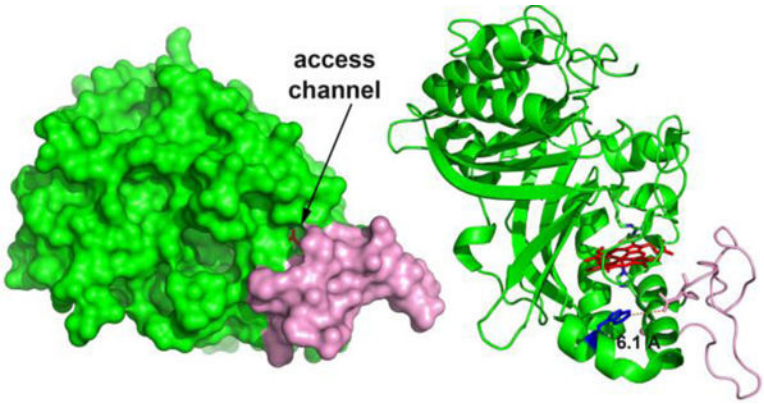

Figure 4.

Crystal structure of *Tc*DyP (PDB 5JXU) in surface (left) and cartoon (right) representations. The loop consisting of residues 277-310 is colored in pink. The heme b, catalytic residues (D220, H312 and R327), W263, and L279 are shown in red, green, blue, and pink sticks.

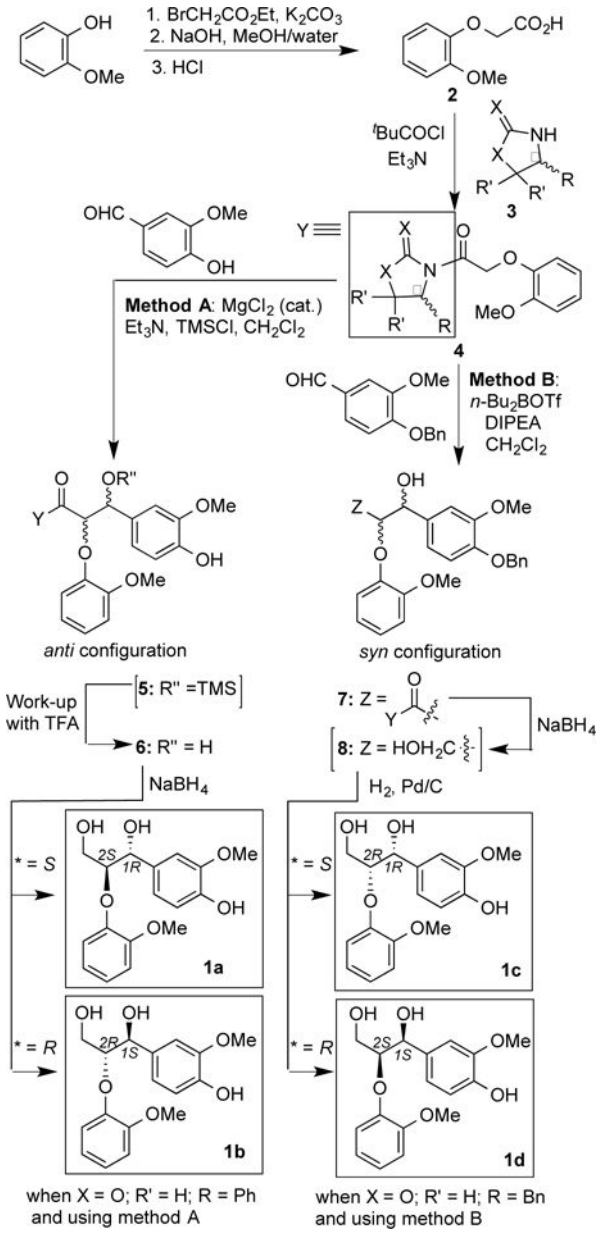

Scheme 1.

Enantioselective synthesis of β-O-4 dilignols[a]

[a]Compounds **5** and **8** were used without purification.

Table 1

Optimization of aldol reactions using method A[a]

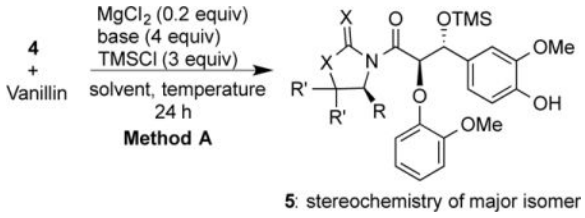

5: stereochemistry of major isomer

entry	compd	base	solvent	diastereoselectivity[b]
1	4a	Et_3N	CH_2Cl_2	78:7:6:9 (rt)
2	4a	Et_3N	CH_2Cl_2	**80:12:4:4**
3	4c	Et_3N	CH_2Cl_2	78:4:16:2 (rt)
4	4e	Et_3N	CH_2Cl_2	72:9:10:9 (rt)
5	4f	Et_3N	CH_2Cl_2	57:27:16 (rt)[c]
6	4g	Et_3N	CH_2Cl_2	31:16:53 (rt)[c]
7	4a	$BuNH_2$	CH_2Cl_2	trace product
8	4a	$PhNH_2$	CH_2Cl_2	no product
9	4a	*i*-Pr_2NH	CH_2Cl_2	73:15:4:8
10	4a	DIPEA[d]	CH_2Cl_2	no product
11	4a	pyridine	CH_2Cl_2	no product
12	4a	DBU[e]	CH_2Cl_2	no product
13	4a	Et_3N	$ClCH_2CH_2Cl$	72:16:7:5
14	4a	Et_3N	EtOAc	76:7:8:9
15	4a	Et_3N	THF	71:2:7:20
16	4a	Et_3N	Et_2O	64:6:14:16
17	4a	Et_3N	toluene	57:6:6:31
18	4a	Et_3N	CH_3CN	no product

[a] Unless indicated, all reactions were carried out at 0 °C;

[b] Diastereoselectivity was determined by HPLC. See SI for details;

[c] Diastereomers were inseparable under this HPLC condition;

[d] Diisopropylethylamine;

[e] 1,8-Diazabicyclo[5.4.0]undec-7-ene.

Table 2

SPR analysis and enzyme assays with *Tc*DyP

parameters		**1a (*1R, 2S*)**	**1b (*1S, 2R*)**	**1c (*1R, 2R*)**	**1d (*1S, 2S*)**
SPR	K_D (μM)	0.166	2.37		2.06
	RU_{max} [a]	35.6	163	ND [c]	68.8
	$Chi^2(RU^2)$ [b]	1.51	0.280		0.575
SA (mU/mg)		232	161	142	215

[a] RU_{max} corresponds to the unconstrained value for the fitted data at saturation, for which the theoretical values are 105 for *Tc*DyP;

[b] The fitting of the observed data to theoretical model is evaluated by Chi^2;

[c] ND: not determined.